JOURNAL OF GEOPHYSICAL RESEARCH, VOL. 112, E08003, doi:10.1029/2006JE002851, 2007

Formation of Mangala Valles outflow channel, Mars: Morphological development and water discharge and duration estimates

Harald J. Leask,[1] Lionel Wilson,[1] and Karl L. Mitchell[1,2]

Received 24 October 2006; revised 3 April 2007; accepted 24 April 2007; published 4 August 2007.

[1] The morphology of features on the floor of the Mangala Valles suggests that the channel system was not bank-full for most of the duration of its formation by water being released from its source, the Mangala Fossa graben. For an estimated typical 50 m water depth, local slopes of sin $\alpha = \sim 0.002$ imply a discharge of $\sim 1 \times 10^7$ m^3 s^{-1}, a water flow speed of ~ 9 m s^{-1}, and a subcritical Froude number of ~ 0.7–0.8. For a range of published estimates of the volume of material eroded from the channel system this implies a duration of ~ 17 days if the sediment carrying capacity of the $\sim 15{,}000$ km^3 of water involved had been 40% by volume. If the sediment load had been 20% by volume, the duration would have been ~ 46 days and the water volume required would have been $\sim 40{,}000$ km^3. Implied bed erosion rates lie in the range ~ 1 to ~ 12 m/day. If the system had been bank-full during the early stages of channel development the discharge could have been up to $\sim 10^8$ m^3 s^{-1}, with flow speeds of ~ 15 m s^{-1} and a subcritical Froude number of ~ 0.4–0.5.

Citation: Leask, H. J., L. Wilson, and K. L. Mitchell (2007), Formation of Mangala Valles outflow channel, Mars: Morphological development and water discharge and duration estimates, *J. Geophys. Res.*, *112*, E08003, doi:10.1029/2006JE002851.

1. Introduction

[2] The Mangala Valles outflow channel system is located in the Memnonia region of Mars, dominated by ancient heavily impact-cratered terrain, and extends from its source in Mangala Fossa, one of the most northerly of the Memnonia Fossae graben, for at least 800 km [*U.S. Geological Survey*, 2003] to the north-northwest (Figure 1). The morphology of the channel system led many workers to conclude that it is the product of one or more episodes of catastrophic water flow [*Hartmann*, 1974; *Sharp and Malin*, 1975; *Chapman and Tanaka*, 1990; *Tanaka and Chapman*, 1990]. *Ghatan et al.* [2005] found that the morphology of the channels could be explained by a single flood episode, whereas by considering the morphology of the source graben, *Leask* [2005] and *Leask et al.* [2007] have argued specifically for two events. Early work placed the formation of the channels within the Late Hesperian to Early Amazonian period [*Scott and Tanaka*, 1986] (cited by *Tanaka* [1986] and *Tanaka and Chapman* [1990]). More recent analyses, generally focusing on the proximal part of the system, by *Chapman and Tanaka* [1993], *Zimbelman et al.* [1994] and *Craddock and Greeley* [1994], as cited by *Ghatan et al.* [2005], place the flood events within the Amazonian.

[3] The source of the Mangala Valles channel system is a gap in the north wall of Mangala Fossa (Figures 2 and 3). The gap marking the water breakout point is located at the lowest part of the north wall of the graben (Figure 4). This location is the lowest point anywhere on either the north or south wall of the graben [*Ghatan et al.*, 2005; *Leask et al.*, 2007], and it is therefore the natural location for water to overflow if the graben had become filled with water. There is some evidence for smaller amounts of water-ice overflow having overtopped the graben in a few other places [*Head et al.*, 2004; *Leask*, 2005; *Leask et al.*, 2007]. A detailed model of the filling, overflow and erosion process is presented by *Leask et al.* [2007], who argue for the water release taking place from an underlying, topographically pressurized aquifer along the boundary faults of the graben.

[4] Each episode of water release is inferred to have accompanied, and continued after, the subsidence of the graben in response to the injection of a dike propagating laterally from the Arsia Mons volcanic system to the east-northeast [*Leask*, 2005; *Leask et al.*, 2007]. *Wilson and Head* [2002] have summarized theoretical and observational evidence for all of the Memnonia Fossae and other graben in this region being the result of faulting and subsidence resulting from the emplacement of a swarm of giant dikes radiating from a mantle magma source beneath Arsia Mons. A volcanically induced origin for the graben is supported by the presence of deposits identified with phreato-magmatic volcanic activity at the eastern end of the graben [*Wilson and Head*, 2004]. In this scenario, water is driven to the surface by the topographic gradient within the aquifer [*Leask et al.*, 2007], the upper surface of which is assumed to mirror closely the surface topography [*Clifford*, 1993]. In contrast, *Hanna and Phillips* [2006] suggest that the graben faulting and aquifer pressurization causing water flow may have been due to the release of stresses during the dike-induced tectonism.

[1] Planetary Science Research Group, Environmental Science Department, Institute of Environmental and Natural Sciences, Lancaster University, Lancaster, UK.
[2] Jet Propulsion Laboratory, Pasadena, California, USA.

0148-0227/07/2006JE002851$09.00

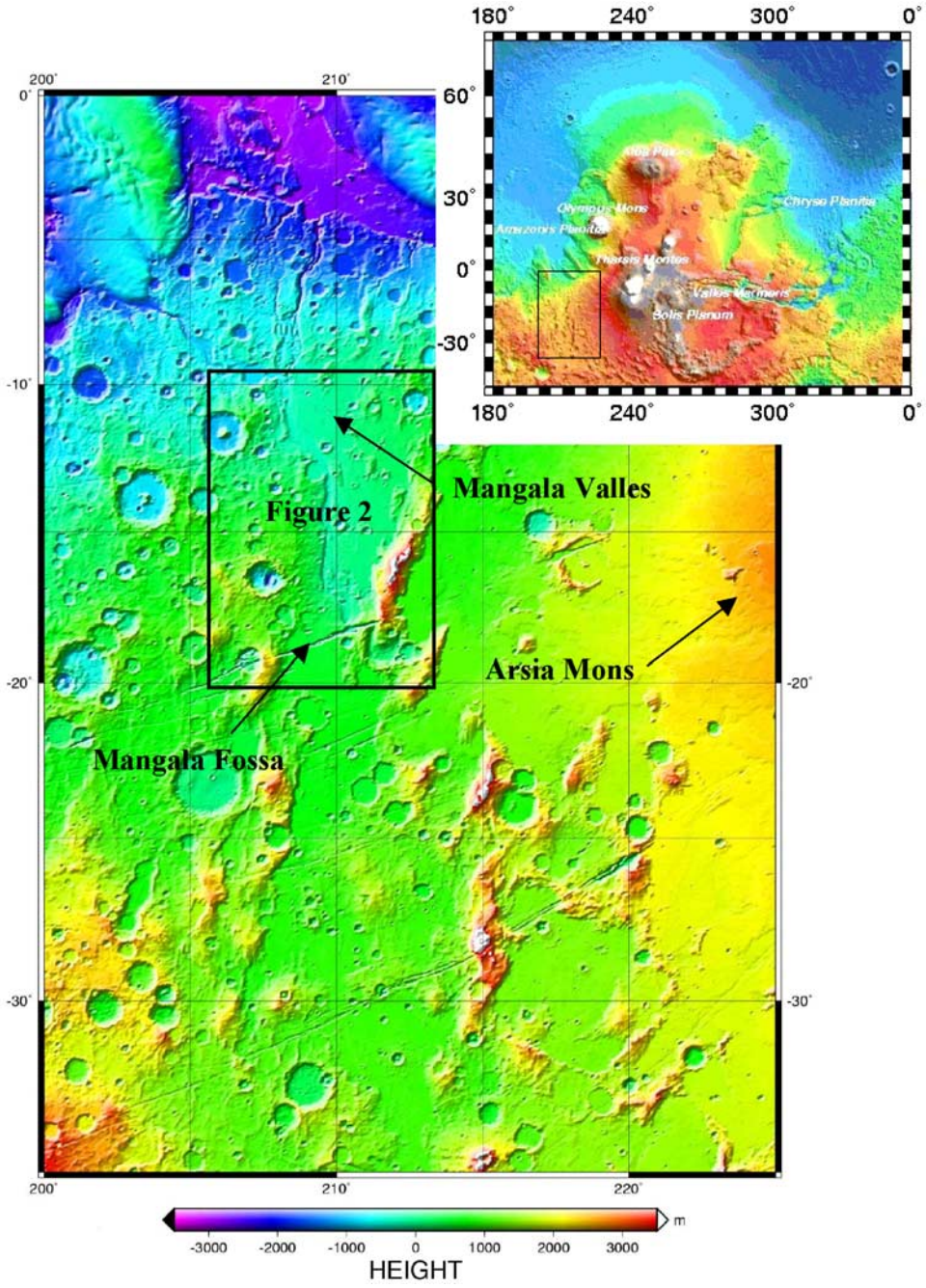

Figure 1. Color-coded MOLA topography of the region containing the Mangala Valles floodplain, the Mangala Fossa source graben, and the highland topography containing the proposed aquifer system feeding the valley. The region shown extends from the equator to 35°S, and from 200°E to 225°E. Inset of Tharsis volcanic area shows location. Box shows location of Figure 2.

[5] Both mechanisms causing water release produce similar initial pressure gradients driving water flow up the fault planes [*Leask et al.*, 2007], but the evolution with time of the pressure gradient, and hence the water discharge rate, is a matter of debate. If the permeability of the underlying aquifer is comparable to that of aquifers in basaltic rocks on Earth, and does not change as water is released, the discharge decreases roughly exponentially, with a timescale that can be a small as tens of minutes [*Carr*, 1979; *Manga*, 2004; *Hanna and Phillips*, 2006]. However, *Leask et al.* [2007] argue that, to explain the amounts of erosion in the larger outflow channels on Mars, either discharges of order 10^7 m^3 s^{-1} must be maintained for times of at least a few weeks, or initial discharges must be very much greater than $\sim 10^7$ m^3 s^{-1}, an option that would require improbably large aquifer permeabilities. Additional support for discharges being maintained at levels of order 10^7 m^3 s^{-1} for much of the duration of the water release comes from calculations of the changes in water depth, speed and temperature with distance from source on Mars [*Bargery and Wilson*, 2006]:

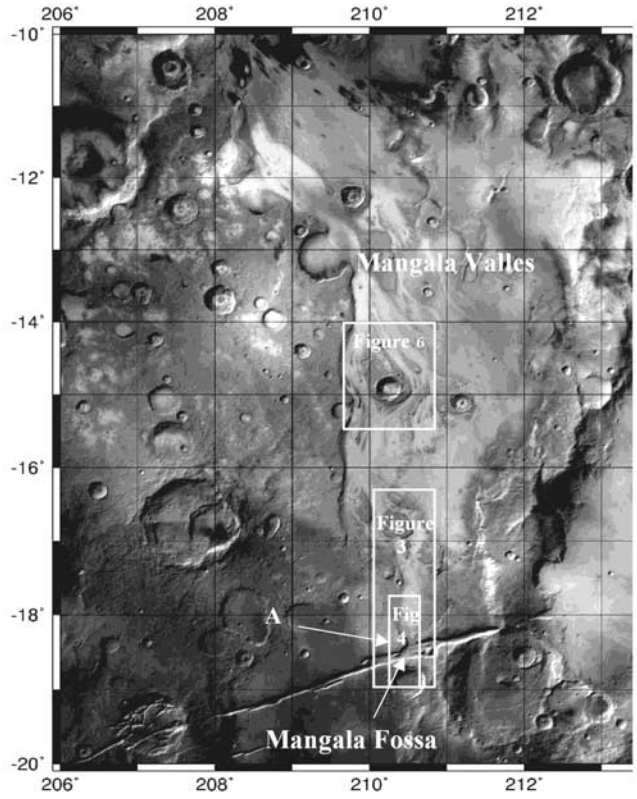

Figure 2. Low-resolution MOC mosaic of Mangala Valles showing outflow channel radiating from a breach in the north wall of Mangala Fossa (A). The region shown extends from 10°S to 20°S, and from 206°E to 213.5°E. Each degree of latitude is ~59.3 km. Boxes show locations of Figures 3, 4, and 6.

a water flood would not remain erosional for the entire ~800 km extent of the channel system at much smaller discharge rates. We therefore support the suggestion of *Carr* [1986] that discharges can be maintained at nearly constant levels for long periods if the aquifer matrix is physically disrupted, with some of the matrix material being elutriated by the water flow.

[6] This paper uses the geometry of the proximal parts of the Mangala Valles channel system to improve previous estimates of the water discharge rate through the channels, focusing on how the discharge can be determined from the depth of water in the channels. If the channel system is the result of two or more events, the implication is that we are deriving information about the last major event.

2. Geomorphology of the Channel System

[7] Figure 5 shows the location of high-resolution images of features present within the Mangala Valles that provide clear evidence that catastrophic floods have occurred there. These include streamlined islands (Figures 3 and 6), terracing (Figures 3, 4, 6, and 7a), chaotic terrain (Figures 3, 6, 7a, and 7b), moats (Figure 7b), and longitudinal lineations (Figures 3, 4, and 7b) [e.g., *Komar*, 1979; *Carr and Clow*, 1981]. Each of these kinds of feature is considered below using low- and high-resolution MOC images and THEMIS visible images. Transverse dunes are also present on the floors of some of the channels (Figure 7b). The morphologies of dunes found elsewhere on Mars have been used to distinguish between aeolian and fluvial formation mechanisms [e.g., *Chapman et al.*, 2003; *Burr et al.*, 2004]. However, we found the morphologies of the dunes on the floors of the Mangala channels to be somewhat ambiguous, possibly implying that they were formed by the superposition of fluvial and aeolian processes, and so we do not consider them further [*Leask*, 2005].

2.1. Streamlined Islands

[8] Streamlined islands are a very distinctive feature of channels on Mars. *Komar* [1983, 1984] showed how streamlined islands commonly occur with their narrow ends pointing down stream, and described how this airfoil shape reduces and minimizes the drag which is exerted by fluid flow. *Komar* [1983] indicated that there is a close correspondence between the airfoil shape of streamlined islands on Mars and of islands in the Channeled Scablands on Earth. These examples provide strong evidence that such features are indicative of water erosion [*Trevena and Picard*, 1978; *Squyres*, 1984; *Burr et al.*, 2002a].

[9] *Rice et al.* [2002] have suggested that some streamlined islands exhibit depositional rather than erosional bed forms, citing Mangala, Ares and Athabasca Valles as examples. *Burr et al.* [2002a, 2002b] and *Burr* [2003] suggest that streamlined mesas at Athabasca Valles were largely the result of sediment deposition behind obstacles during fluid flow, followed by partial erosion of the deposited material [*Burr*, 2005]. Given the possibility that there may have been two flood events in the Mangala Valles [*Leask et al.*, 2007], the present morphology of the streamlined islands may be a complex superposition of erosional and depositional episodes.

2.2. Terraces

[10] The terraces present in Mangala Valles (Figures 3, 4, 6, and 7a) are similar to those found in other outflow channels on Mars [*Baker and Kochel*, 1978, 1979; *Mars Channel Working Group*, 1983; *Carr*, 1986; *Chapman and Scott*, 1989; *Leask*, 2005; *Leask et al.*, 2006a] as well as in the Channeled Scablands on Earth [*Baker and Kochel*, 1979] and give some indication of the pattern of erosion that occurred during the flood events [*Nummedal et al.*, 1976; *Masursky et al.*, 1977; *Leask*, 2005; *Leask et al.*, 2006a]. Specifically, terraces indicate changing water levels during erosion of the channels. Unfortunately the amount of erosion has been so great that it is very hard to establish reliable positions of the channel floor in the very early stages of flooding from the present topography.

2.3. Moats

[11] At Mangala Valles, high-resolution MOC images show the presence of moats (Figure 7b) around island-like outcrops of relatively resistant material. Less-resistant material surrounding the outcrops has been eroded and removed, and some deposition has occurred on the lee side. The morphology of these features is similar to that seen on the floors of the Grjótá Valles channels, interpreted by *Burr and Parker* [2006] to represent highstanding features first embayed by lava flows and then subjected to fluvial

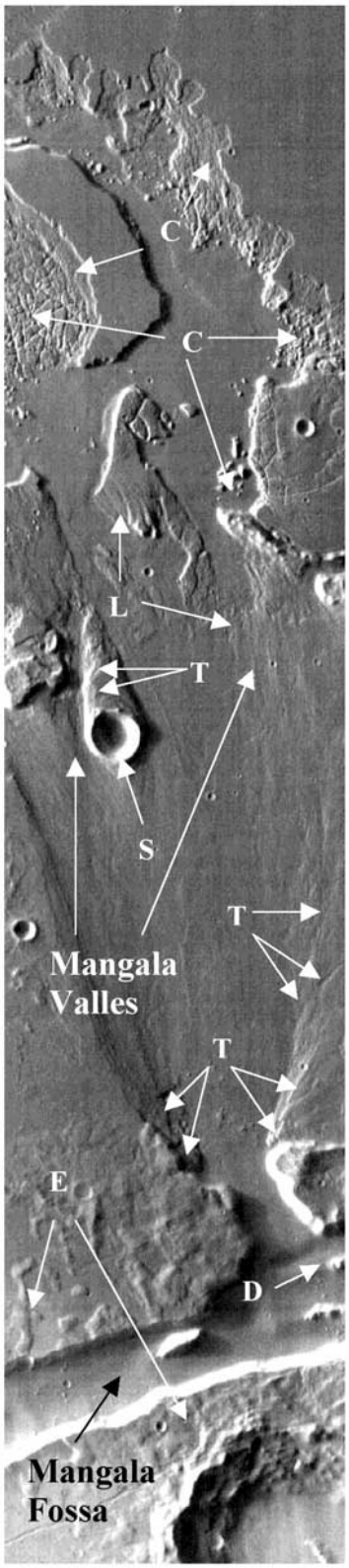

erosion. The inference is that the lava is more resistant to erosion than the material forming the highstanding features, so that they are preferentially removed leaving a depression marking their original extents. If this origin is relevant to the Mangala Valles features, it is consistent with the interpretation that there were two flood episodes [*Leask et al.*, 2007], lava being emplaced on the first channel floor between the two events. Whatever the details, we regard these largely erosional features as important qualitative indicators of water flow through this area [*Leask*, 2005], but we have not devised a way of using them quantitatively.

2.4. Chaotic Terrain

[12] Chaotic terrain similar to that found elsewhere on Mars occurs in small amounts within Mangala Valles (Figures 3, 7a, and 7b). Some discrete areas of chaotic terrain on Mars form the sources of outflow channels and these are probably formed by sudden discharge of water from beneath the cryosphere, which results in the collapse of overlying terrain [*Baker and Kochel*, 1979; *Baker et al.*, 1991; *Chapman et al.*, 2003]. In some cases the trigger for this may be the intrusion of a sill [*Leask et al.*, 2006b] which applies stresses to the cryosphere rocks and also enhances the local heat flow at shallow depth, melting some of the cryosphere ice. The combination of these factors causes fracturing of the cryosphere, thus allowing pressurized water to rise into the fractures [*Masursky et al.*, 1977; *Theilig and Greeley*, 1979; *Baker et al.*, 1991; *Chapman and Tanaka*, 2002; *Leask*, 2005]. In a study of Ravi Vallis, *Coleman* [2005] has pointed out that where a channel floor is undergoing extensive erosion the removal of some of the overlying cryosphere may itself be enough to allow pressurized water from a localized aquifer to break through to the surface. This may explain of the patches of chaos shown in Figure 3. The location of the chaotic terrain will then depend on the strength of the cryosphere materials as well as the presence or absence of available water. Once localized water breakout of this kind had started, it is possible that it continued long after cessation of the water supply from the main source in Mangala Fossa, enlarging the initial area of breakout [*Baker and Kochel*, 1979; *Schultz et al.*, 1982; *Laity and Malin*, 1985; *Kochel and Piper*, 1986; *Chapman and Scott*, 1989; *Luo et al.*, 1997].

2.5. Longitudinal Lineations

[13] Longitudinal lineations are present in Mangala Valles as previously asserted by *Sharp and Malin* [1975], *Carr and Clow* [1981], and *Nummedal and Prior* [1981]. These features (Figures 3, 4, and 7b) show clear evidence that

Figure 3. THEMIS IR (100 m resolution) image I05511003 of Mangala Valles showing the area where there is a breach, ~5 km wide, in the north wall of Mangala Fossa. Streamlined islands (S), longitudinal lineations (L), terracing (T), and chaotic terrain (C) are present downchannel from the breakout point. Note that ejecta (E) from the impact crater on the south side of the graben is present on both sides of the graben, but is not present on the floor of the graben, suggesting that the crater must be older than the last flood event. Top of dike (D) is located near to the gap. North is to the top.

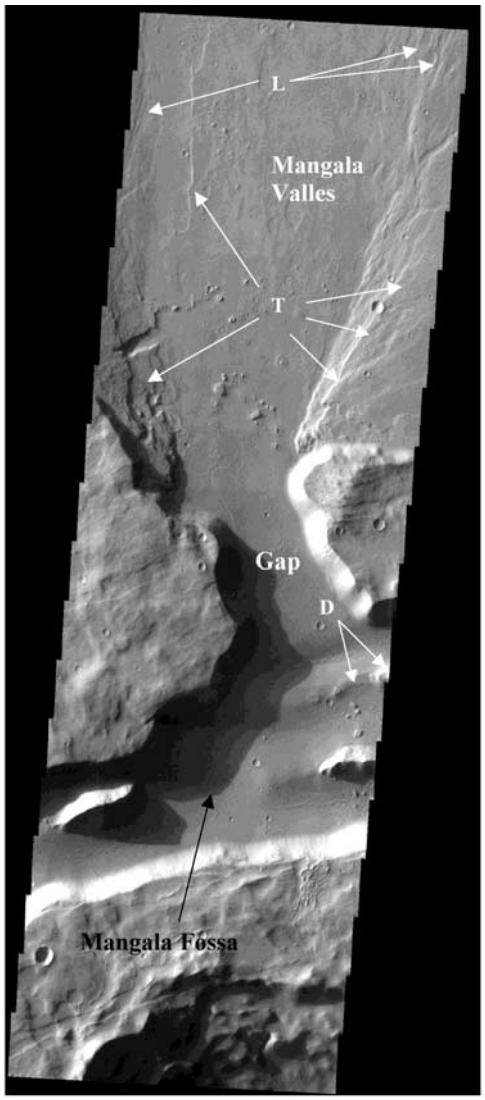

Figure 4. THEMIS-VIS (100 m resolution) close-up image V04762003 of Mangala Valles showing the area where there is a breach in the north wall of Mangala Fossa. Longitudinal lineations (L) and terracing (T) are present down-channel from the breakout point which is ~5 km wide. Top of dike (D) is located near to the gap. North is to the top.

the local bed rock has been eroded. Furthermore, the scour marks on the channel floors in both areas are orientated in the direction of fluid flow as indicated by channel boundaries [*Leask*, 2005]. This close and local topographic control is in marked contrast to the more uniform and slowly changing orientations of lineations caused by aeolian processes, for example, the yardangs described by *Edgett and Malin* [2000].

2.6. Implications of Morphology

[14] The various lines of evidence outlined above lead us to conclude that erosion dominated over deposition in the proximal parts of the Mangala Valles channel system. We therefore consider it reasonable to use the present topography of the deepest parts of the channels to infer water flow rates and minimum water volumes involved in the most recent flood event in this area. Topographic profiles were constructed across the channels at 0.1 degree intervals between 17.5 and 16.5 degrees south using MOLA altimetry data. These are shown in Figure 8a and their locations are indicated on Figure 8b. The profiles clearly show that the floors of the main channels are dissected into deeper subchannels, and a major issue as regards water flow through the system is whether water was confined to individual subchannels or flooded the main channels to a great enough depth to interconnect the subchannels. We explore both possibilities in the next section.

3. Estimation of Water Discharge Rate

[15] We estimate the volume flux, V, of water though any one subchannel from

$$V = u\ d\ w, \tag{1}$$

where u is the mean speed of water in the channel, d is the depth of the water and w is the mean width of the channel. Unless both banks of a channel are vertical, the mean width of a channel with a given cross-sectional profile will depend on the depth to which it is filled and must be evaluated numerically from the profile. The mean speed of the water is given by

$$u = [(8\ d\ g \sin\alpha)/f]^{1/2}, \tag{2}$$

where g is the acceleration due to gravity, 3.72 m s^{-2}, α is the slope of the channel bed, and f is the dimensionless Darcy-Weisbach bed friction factor, a function of the grain size distribution of the bed material, the water depth and the flow regime, specified in equations given by *Bathurst* [1993]. *Wilson et al.* [2004] used measurements of rock size distributions on the surface of Mars made by *Golombek and Rapp* [1997] and *Golombek et al.* [2003] to implement the equations of *Bathurst* [1993] in a spreadsheet computer program. *Kleinhans* [2005] pointed out that *Wilson et al.* [2004] misinterpreted how the rock size distributions were specified by *Golombek and Rapp* [1997] and *Golombek et al.* [2003], resulting in a ~10% overestimate in all of the flow speeds calculated. We have corrected the computer program devised by *Wilson et al.* [2004] to take account of this. We used *Wilson et al.*'s [2004] equation (15), applicable to boulder-dominated channel beds, but corrected the parameter D_{84}, the clast size exceeded by 16% of the bed material, from the value 0.164 m originally used by *Wilson et al.* [2004] to the value 0.48 m deduced by *Kleinhans* [2005]. Note that equation (2) above is applicable to turbulent flow, always appropriate for outflow channel floods [*Wilson et al.*, 2004], and does not explicitly involve the fluid density (though there may be second-order effects of the fluid density on f). Thus the equation is applicable to sediment-laden, as well as sediment-free, water flows as long as the sediment load does not become so large that turbulence is damped out or the rheology of the flow becomes non-Newtonian [*Bargery et al.*, 2005]. Thus, given measurements of water depth, channel floor slope and channel profile, we can calculate discharge.

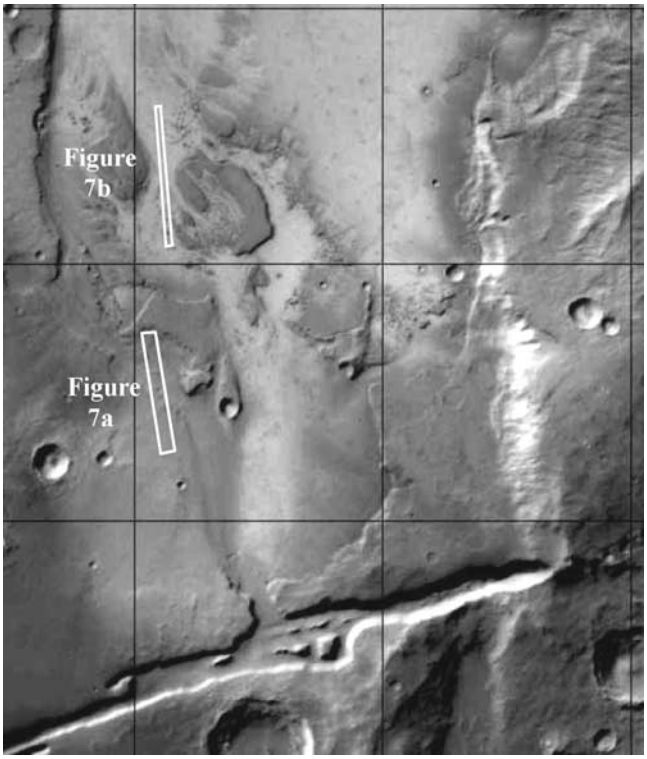

Figure 5. Overview of area showing locations of Figures 7a and 7b.

[16] We showed in Figure 8a how MOLA data can be used to derive cross-sectional profiles of subchannels. Enlargements of these profiles (e.g., Figure 9) were examined to determine the number of subchannels in each, and this was found to range from 1 to 6. It was noted that local subchannel depths below the tops of the divides between channels were commonly ~50 m, implying that a water depth of this magnitude would have corresponded to the subchannels being individually bank-full. We consider it unlikely that the water depth was ever very much greater than ~50 m, otherwise a smaller number of wider subchannels would have formed, and infer that 150 m is a likely upper limit on water depth. This 50- to 150-m range of water depths was therefore used as a starting point for calculating the discharge. The channel system at each cross section in Figure 9 was conceptually flooded with water, starting from each subchannel floor and increasing the water depth in increments of 50 m. Measurement of the horizontal channel width at each increment of depth allowed the mean channel width for any given water depth to be found. The average channel floor slope between any two locations along its path was found by taking the difference between the mean floor levels. The average slope between 16.5°S and 17.5°S latitude, a distance of ~68 km along the average path of the channel system, was $\sin \alpha = 0.002$.

[17] Table 1 shows the results for the channel system at 16.7 °S, giving the volume fluxes for the individual subchannels and the total for the cross section. Table 2 summarizes the corresponding total fluxes for all of the 11 cross sections analyzed. Clearly, if the water depth were large enough to cause the entire channel system to approach bank-full, the water volume flux could be inferred to have been approaching 10^8 m^3 s^{-1}. However, erosion must have been taking place in the channels, and no channel subject to erosion can remain bank-full unless the water volume flux flowing through it increases with time, an unlikely circumstance for a water flood draining an aquifer system as is inferred to be the case here [*Tanaka and Chapman*, 1990; *Zimbelman et al.*, 1992; *Ghatan et al.*, 2005; *Leask et al.*, 2007]. We take the presence of numerous subchannels with depths commonly of ~50 m to imply that the water depth was of this order in the region studied for most of the duration of the flood, implying that the flux was close to 1×10^7 m^3 s^{-1} for much of the duration.

[18] If there were no sources or sinks of water in the channel system one would expect the total flux to be the same at all cross sections at any given time, apart from some reduction due to infiltration or evaporation from the water surface. Infiltration is likely to be negligible on Mars given the low surface and shallow subsurface temperatures [*Clifford and Parker*, 2001], but evaporation is relatively much more important on Mars than on Earth because of the low atmospheric pressure [*Wallace and Sagan*, 1979]. The likely evaporative reduction in water depth and flow conditions over the ~70 km channel length studied here can be estimated using the mass loss rate of molecules from the water surface, controlled by the temperature-dependent vapor pressure of the water. The calculation, outlined by

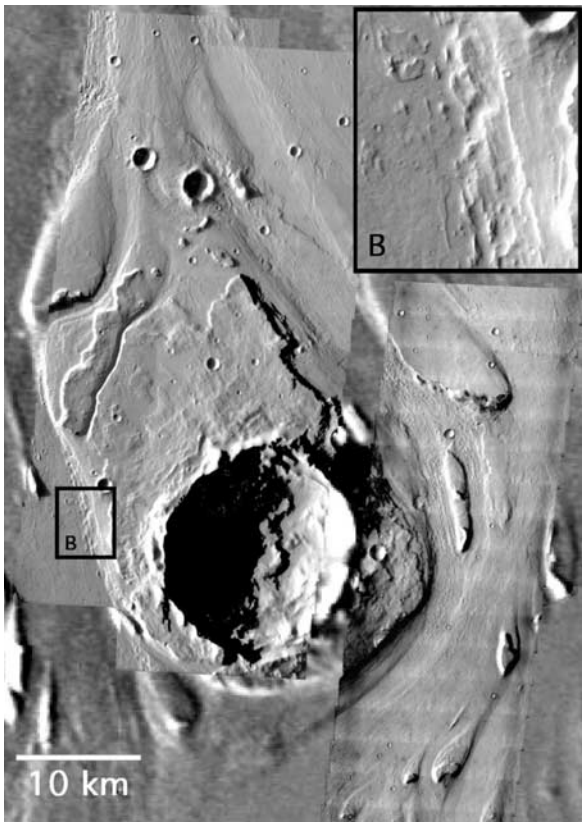

Figure 6. THEMIS images V01429002, V04787002 and V05898002, superimposed on Viking mosaic, showing large streamlined island in Mangala Valles located at about 15°S, and between 210°E and 211°E. Box indicated by B is enlarged at upper right to show details of terraces.

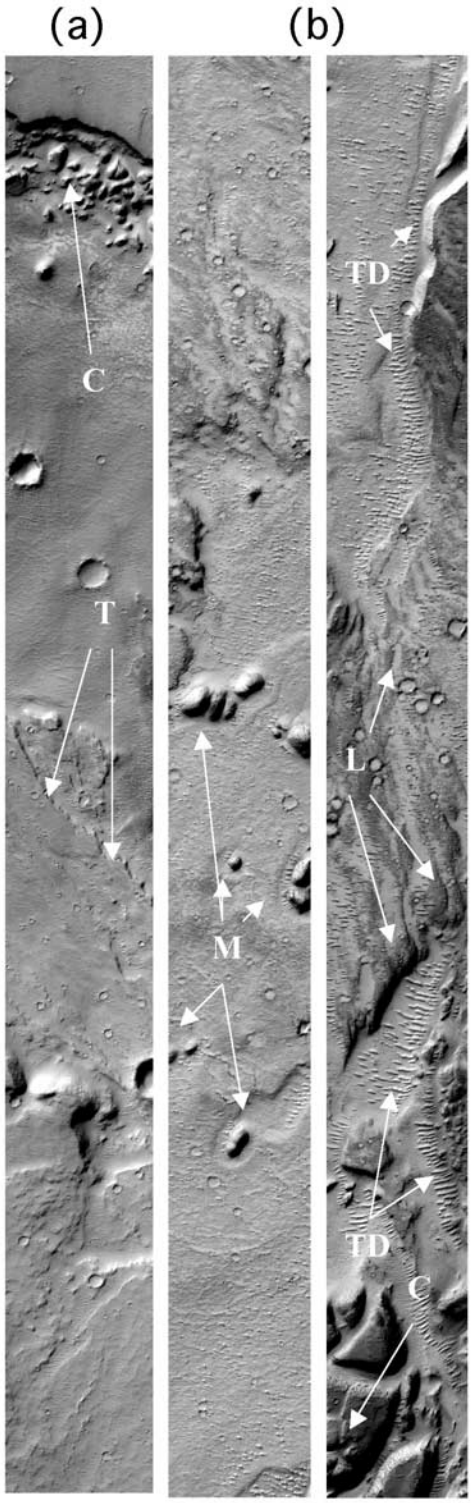

Figure 7. (a) Part of narrow angle MOC image m1900218 of Mangala Valles, latitude 17.50°S, longitude 209.97°E showing terracing (T) and chaotic terrain (C). North is to the top; image width is 2810 m. (b) Part of narrow angle MOC image m2300637 of Mangala Valles, latitude 16.68°S, longitude 209.96°E showing longitudinal lineations (L), transverse dunes (TD), chaotic terrain (C), and moats (M). North is to the top; image width is 1490 m. Left frame of pair is northern half of image, and right frame is southern half.

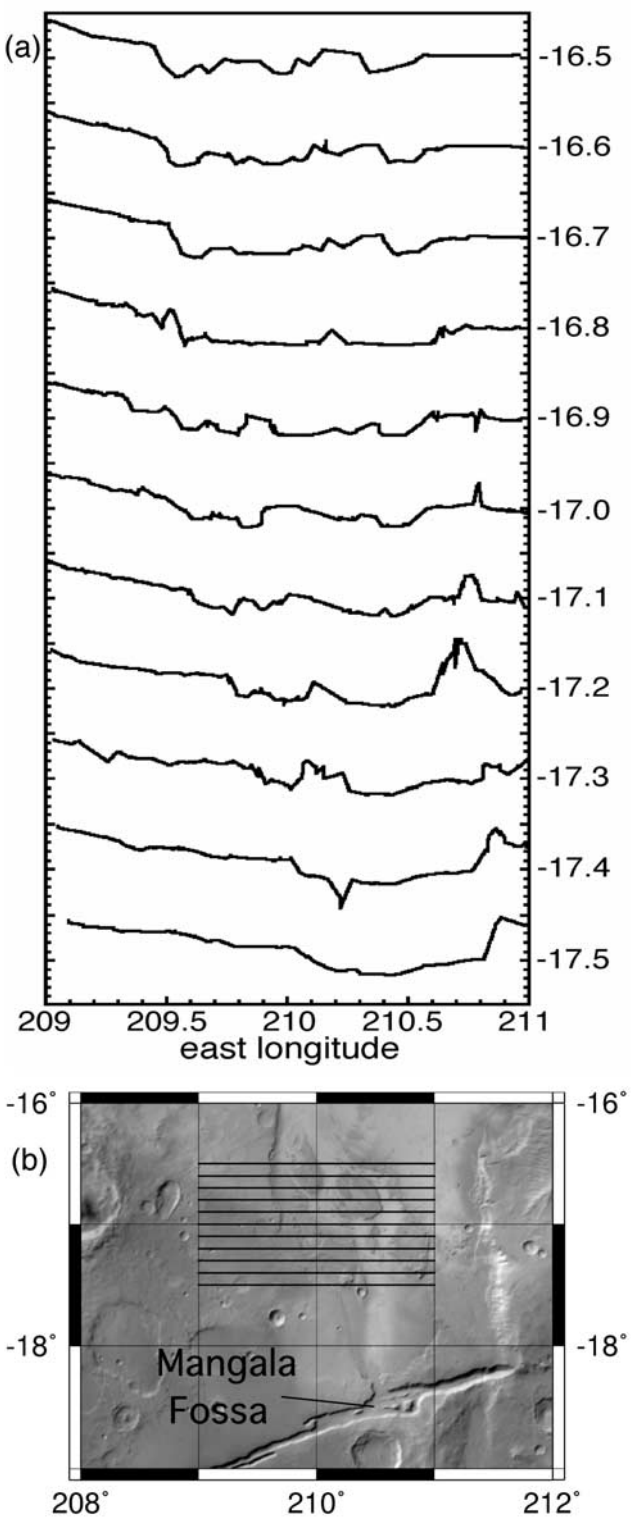

Figure 8. (a) MOLA cross sections of the 11 channels examined at Mangala Valles. Numbers to right of profiles indicate latitudes. Small tick marks on vertical axis are 100-m-height increments. Each degree of east longitude is about 56.7 km. (b) Locations of profiles.

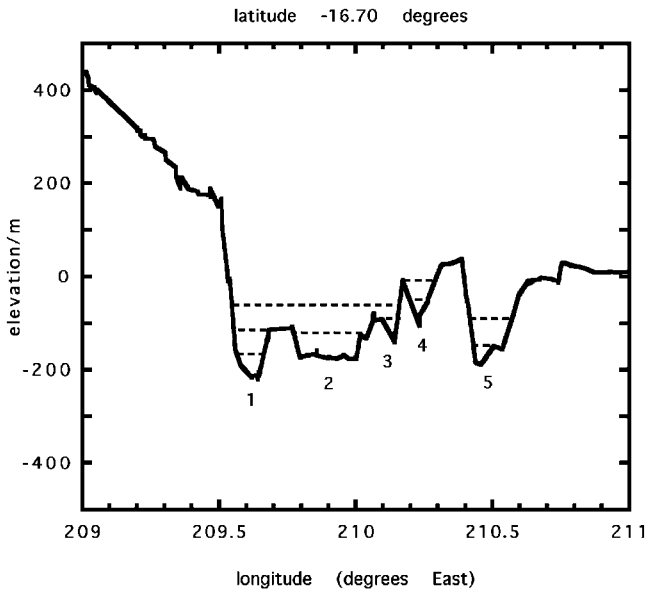

Figure 9. MOLA topography of subchannels (numbered 1 to 5) of Mangala Valles at latitude 16.70°S. Each degree of latitude is ~59.3 km. Where channel bank slopes are fairly uniform, water depth increments at ~50-m intervals are shown as dotted lines. In some subchannels, depth increments change so that a water level can be placed at any point where a sudden change in channel width occurs. Water depths are incremented separately from the bottom of each subchannel, and incrementing stops when the level would cause water to spill sideways from any subchannel to an adjacent one.

Bargery et al. [2005] and to be described in detail elsewhere, requires knowledge of the water temperature on release from the subsurface which, in a study of the source graben, *Leask et al.* [2007] show could have been as much as ~40°C. Starting from this temperature, the water would have cooled to 0°C in about 31 min [*Bargery et al.*, 2005]. For an initial water depth in the range ~50 to 100 m and typical flow speed of ~12.5 m s^{-1} (see Table 1), it would have traveled ~23 km in this time. By the time the water reached the start of the region studied at 17.5°S it would have traveled ~60 km from the source graben at ~ 18.5°S (see Figure 2) requiring a further ~49 min, by which time calculations to be described elsewhere show that up to ~28% of the water would have frozen to form ice crystals. The total depth reduction due to water evaporation would have been ~5.5 m, i.e., about 10% of the typical value. This would have produced about a 5% reduction in velocity and hence volume flux, much smaller than any variation that we might be able to detect.

[19] Table 3 shows the values of the Froude number, *Fr*, defined by

$$Fr = u/(gd)^{1/2}, \tag{3}$$

for flow in the channel system between 17.5 and 16.5°S for water depths of ~50 m (actually close to 51.8 m due to the scale of the graphs of the profiles used) and 150 m. The values lie in the range 0.69 to 0.81 for the local channel floor slope of sin α = 0.002, and in the range 0.44 to 0.52 for the regional slope of sin α = 0.00082 between the channel source and 16.5°S. They are all clearly subcritical, confirming that the equations used to specify the flow conditions and define the friction factors are valid for the flow regime.

4. Channel Erosion, Water Volume, Flood Duration, and Aquifer Geometry

[20] Using our best estimate of the water depth, Table 2 gives our average value for the volume flux of water flowing through the Mangala channel system during most of the duration of its erosion as ~1 × 10^7 m^3 s^{-1}. The total volume of material eroded from the channel system has been estimated by *Hanna and Phillips* [2006] as 5700 km^3, a value similar to the ~5000 km^3 estimate of *Tanaka and Chapman* [1990]. However, *Ghatan et al.* [2005] found the total eroded volume to lie between 13,000 and 20,000 km^3. We adopt 10,000 km^3 in what follows. Using the suggestion of *Komar* [1980] that the maximum volume fraction of sediment that could be carried by a water flood is ~40%, this implies that the minimum volume of water that must have flowed through the Mangala Valles was ~15,000 km^3. At a discharge of 1 × 10^7 m^3 s^{-1} this would require ~17 days. However, there is no guarantee that the maximum possible sediment load was carried. A sediment load in of 20% would imply a minimum water volume of 40,000 km^3 and a duration of ~46 days, and a sediment load in of 10% would imply a minimum water volume of 90,000 km^3 and a duration of ~104 days. Table 4 summarizes water volumes and durations for sediment loads ranging from the ~40% upper limit down to 5%. It is clear that the required water volume is at least 20,000 km^3 and could be as much as 100,000 km^3.

[21] Typical total depths of erosion in the channels in the region studied here (Figure 8) are ~200 m. Using this value and the above duration estimates we give the corresponding erosion rates in Table 4: These range from ~1 to ~12 m/day. There have been few attempts to derive bed erosion rates for outflow channels on Mars, though estimates for a combination of thermal and mechanical erosion derived from laboratory experiments of up to ~1 m/day were given by *Costard et al.* [1999]. Using a method similar to that described here, *Leask et al.* [2006a] found erosion rates for the near-critical to supercritical water flood in Ravi Vallis in the range 20 to 100 m/day, about a factor of 10 greater than the rates found here for the Mangala Valles.

[22] The area occupied by the aquifer supplying the water that was released through the Mangala Fossa graben to feed the Mangala Valles can be estimated as follows. Using a simple model of the geothermal heat flow and the Mars crust models of *Clifford* [1993] and *Hanna and Phillips* [2005], *Leask et al.* [2007] calculated that the aquifer was probably located at depths between ~4 and ~10 km and had a mean porosity of ~4%. To accommodate the range of water volumes found above, ~20,000 km^3 to ~100,000 km^3, the required areas are then ~80,000 to ~400,000 km^2. There are two options for the location of the aquifer system.

Table 1. Data for Mangala Valles Channels at Latitude −16.70°[a]

	Water Depth		
	Increment 1	Increment 2	Increment 3
Channel 1			
Depth, Individual Depth Increment/m	51.8	51.8	46.6
Depth, Running Total of Increments/m	51.8	103.6	150.2
Average Width, Individual Increment/km	4.22	6.32	35.84
Mean Channel Width to Running Total Depth/km	4.22	5.27	14.76
Darcy-Weisbach Friction Factor	0.0336	0.0273	0.0246
Mean Water Speed to Running Total Depth/(m/s)	9.60	15.07	19.11
Discharge to Running Total Depth/(m^3/s)	2.10×10^6	8.23×10^6	4.24×10^7
Channel 2			
Depth, Individual Depth Increment/m	51.8	10.4	
Depth, Running Total of Increments/m	51.8	62.2	
Average Width, Individual Increment/km	13.7	16.9	
Mean Channel Width to Running Total Depth/km	13.7	14.2	
Darcy-Weisbach Friction Factor	0.0336	0.0318	
Mean Water Speed to Running Total Depth/(m/s)	9.60	10.82	
Discharge to Running Total Depth/(m^3/s)	6.82×10^6	9.57×10^6	
Depth, Individual Depth Increment/m	51.8	10.4	
Channel 3			
Depth, Individual Depth Increment/m	51.8		
Depth, Running Total of Increments/m	51.8		
Average Width, Individual Increment/km	2.11		
Mean Channel Width to Running Total Depth/km	2.11		
Darcy-Weisbach Friction Factor	0.0336		
Mean Water Speed to Running Total Depth/(m/s)	9.60		
Discharge to Running Total Depth/(m^3/s)	1.05×10^6		
Channel 4			
Depth, Individual Depth Increment/m	51.8	51.8	
Depth, Running Total of Increments/m	51.8	103.6	
Average Width, Individual Increment/km	2.11	5.27	
Mean Channel Width to Running Total Depth/km	2.11	3.69	
Darcy-Weisbach Friction Factor	0.0336	0.0273	
Mean Water Speed to Running Total Depth/(m/s)	9.60	15.07	
Discharge to Running Total Depth/(m^3/s)	1.05×10^6	5.76×10^6	
Channel 5			
Depth, Individual Depth Increment/m	41.4	114.0	
Depth, Running Total of Increments/m	41.4	155.4	
Average Width, Individual Increment/km	2.64	9.49	
Mean Channel Width to Running Total Depth/km	2.64	7.66	
Darcy-Weisbach Friction Factor	0.0361	0.0244	
Mean Water Speed to Running Total Depth/(m/s)	8.29	19.52	
Discharge to Running Total Depth/(m^3/s)	9.05×10^5	2.32×10^7	
Total discharge/(m^3/s), all channels bank-full (up to ∼150 m deep)	8.2×10^7		
Total discharge/(m^3/s), water ∼52 m deep	1.2×10^7		

[a]Water depths in channel are incremented in uniform (51.8 m) steps where bank slopes are fairly uniform, but other depth levels are used when needed to coincide with sudden changes in channel width. See Figure 9.

Table 2. Total Volume Fluxes for Two Water Depths at Mangala Valles

Latitude	Water Depth ∼51.8 m	Water Depth Lesser of Bank Full or 150 m
−17.50	5.24×10^6	5.84×10^7
−17.40	5.24×10^6	6.64×10^7
−17.30	5.76×10^6	4.81×10^7
−17.20	1.68×10^7	5.98×10^7
−17.10	9.39×10^6	5.99×10^7
−17.00	6.97×10^6	5.57×10^7
−16.90	1.79×10^7	9.78×10^7
−16.80	2.36×10^7	1.52×10^8
−16.70	1.19×10^7	8.20×10^7
−16.60	1.26×10^7	6.18×10^7
−16.50	5.47×10^6	5.40×10^7
Average volume fluxes	1.10×10^7	7.24×10^7
Standard deviations	0.62×10^7	2.99×10^7

Table 3. Calculation of Friction Factors, Water Flow Speeds, and Froude Numbers for ∼50 m and 150 m Water Depths in the Part of the Mangala Valles Analyzed Using Two Different Slope Tangents, the Regional Value 0.00082, and the Typical Local Value in Channels, 0.002[a]

Depth, m	Slope	Friction Factor	Speed, m/s	Froude Number
∼52	0.00082	0.0337	6.10	0.441
150	0.00082	0.0246	12.22	0.516
∼52	0.002	0.0337	9.53	0.689
150	0.002	0.0246	19.09	0.806

[a]Friction formulae for boulder-dominated channel beds are used.

Table 4. Water Volumes, Flood Durations, and Bed Erosion Rates Implied by Various Assumptions About the Sediment-Carrying Capacity of the Mangala Valles Flood

Sediment load/ volume%	Volume of water/km^3	Duration of flood/days	Bed erosion rate/(m/day)
40	15,000	17	11.5
30	23,000	27	7.4
20	40,000	46	4.3
10	90,000	104	1.9
5	190,000	220	0.9

To the south of the graben, the topography defines a valley ~400 km wide and at least 1000 km long (see Figure 1). Although this region has the required area and its slope is in the required sense (down to the north), the total elevation change is only ~1 km, and if the top of the aquifer mirrors the surface topography, this is not enough to cause a substantial fraction of the aquifer thickness to empty to the surface. There is the additional complication that several more graben of the Memnonia and Sirenum Fossae swarms run roughly E-W across this area, and if these are underlain by dikes as inferred by *Wilson and Head* [2002] and *Leask et al.* [2007] then, depending on their relative timing, the intrusions would have acted as aquicludes segmenting the aquifer system beneath the valley. We therefore concur with earlier suggestions [e.g., *Tanaka and Chapman*, 1990; *Zimbelman et al.*, 1992], that the aquifer system extends mainly eastward under the flanks of Arsia Mons, where an ample area and topographic head is available.

5. Discussion

[23] We have obtained our flux values by using the morphology to estimate the depth of the water at each of a series of cross sections through the channel system. A more detailed analysis would model the water flow with an energy surface superimposed onto the digital topography and would use continuity of the volume flux as an input to solving the system. However, owing to the nonuniformity of MOLA altimetry coverage at the low latitude of the Mangala Valles we do not consider the present level of topographic detail to be enough to justify this approach. Our discharge estimates are a little greater than those obtained by *Komar* [1979] using earlier Viking data sources for the channel topography and by *Ghatan et al.* [2005] who based their analysis on the morphology of a small part of the system, the notch through which water flowed from the source graben to feed the channels.

[24] We commented that the amount of evaporation that would have occurred while water was crossing the region studied here would have been relatively small. However, we note that at our estimated flow speeds (Tables 1 and 3) water would have required ~90 min to travel down the part of the channel system studied, and the conditions in the water during this period would have depended heavily on whether the ice crystals forming in the flow were able to collect at the flow surface to form an ice raft or remained completely dispersed throughout the flow. In the former case, the surface of the ice raft would have rapidly cooled to the ambient atmospheric temperature, greatly inhibiting evaporation [*Wallace and Sagan*, 1979], heat loss and further ice formation; in the latter case, significant additional ice formation could have begun to change the rheology of the water and reduce its flow speed, probably changing its erosive capability and possibly leading to sediment deposition on the floor of the channel [*Bargery et al.*, 2005]. While these issues do not impinge too strongly on the discharge estimates for the region studied here, they would become progressively more important for any analysis of the more distal part of the channel system.

6. Summary

[25] 1. Of the various features providing evidence of water flow in Mangala Valles, initiated by dike emplacement events forming the Mangala Fossa source, we regard streamlined islands, moats and terraces as unambiguous; patches of chaotic terrain and longitudinal lineations as suggestive; but transverse dunes as less convincing.

[26] 2. The morphology of the floor of Mangala Valles, specifically the presence of subchannels on the main channel floor, suggests that the water depth in the channel system was of order 50 m for most of the duration of the erosion event, though initially the channel system may have been bank-full.

[27] 3. If the channel system had been bank-full, the regional slope of sin $\alpha = 0.00082$, combined with the water depth, would have led to a discharge of about 10^8 m^3 s^{-1}.

[28] 4. Under what we consider to be the more typical flow conditions, the local floor slopes of typically sin $\alpha = 0.002$ combined with the ~50 m water depths imply a discharge of close to 1×10^7 m^3 s^{-1}.

[29] 5. The region studied (16.5 to 17.5 °S) is sufficiently close to the water source that changes in flow conditions due to evaporation and freezing of water under Martian environmental conditions were probably not important.

[30] 6. The Froude numbers for the flow conditions, ~0.43 to 0.52 for possible early bank-full flow and ~0.68 to 0.81 for most of the discharge, were all clearly subcritical.

[31] 7. At a discharge of 1×10^7 m^3 s^{-1}, the ~200 m of erosion of the channel system would have required 17 days if the sediment-carrying capacity of the 15,000 km^3 of water required had been ~40% by volume; for a 20% sediment load the duration would have been ~46 days and the water volume required would have been ~40,000 km^3. Implied bed erosion rates lie in the range ~1 to ~12 m/day.

[32] **Acknowledgments.** L. W. and K. L. M. were supported in part by PPARC grant PPA/G/S/2000/00521. K. L. M. also acknowledges support by the NRC in the form of a Postdoctoral Research Associateship, carried out at the Jet Propulsion Laboratory, California Institute of Technology, under a contract with the National Aeronautics and Space Administration. We thank J. W. Head, G. J. Ghatan, and K. J. Beven for useful discussions, and reviewers Devon Burr and Jeffrey Andrews-Hanna for their many helpful suggestions for improvements.

References

Baker, V. R., and R. C. Kochel (1978), Morphological mapping of Martian outflow channels, *Proc. Lunar Planet. Sci. Conf.*, *9th*, 3181–3192.

Baker, V. R., and R. C. Kochel (1979), Martian channel morphology: Maja and Kasei Valles, *J. Geophys. Res.*, *84*(B14), 7961–7983.

Baker, V. R., R. G. Strom, V. C. Gulick, J. S. Kargel, G. Komatsu, and V. S. Kale (1991), Ancient oceans, ice sheets and the hydrological cycle on Mars, *Nature*, *352*, 589–594.

Bargery, A. S., and L. Wilson (2006), Modelling water flow with bedload on the surface of Mars, *Lunar Planet. Sci.* [CD-ROM], *XXXVII*, abstract 1218.

Bargery, A. S., L. Wilson, and K. L. Mitchell (2005), Modelling catastrophic floods on the surface of Mars, *Lunar Planet. Sci.* [CD-ROM], *XXXVI*, abstract 1961.

Bathurst, J. C. (1993), Flow resistance through the channel network, *in Channel Network Hydrology*, edited by K. Beven and M. J. Kirkby, pp. 69–98, John Wiley, Hoboken, N. J.

Burr, D. M. (2003), Temporary ponding of floodwater in Athabasca Vallis, *Mars, Lunar Planet. Sci.* [CD-ROM], *XXXIV*, abstract 1066.

Burr, D. M. (2005), Clustered streamlined forms in Athabasca Valles, Mars: Evidence for sediment deposition during floodwater ponding, *Geomorphology*, *69*(1–4), 242–252.

Burr, D. M., and A. H. Parker (2006), Grjotá Valles and implications for flood sediment deposition on Mars, *Geophys. Res. Lett.*, *33*, L22201, doi:10.1029/2006GL028011.

Burr, D. M., A. S. McEwen, and S. E. H. Sakimoto (2002a), Recent aqueous floods from the Cerberus Fossae, *Geophys. Res. Lett.*, *29*(1), 1013, doi:10.1029/2001GL013345.

Burr, D. M., J. A. Grier, A. S. McEwen, and L. P. Keszthelyi (2002b), Repeated aqueous flooding from the Cerberus Fossae: Evidence for very recently extant, deep groundwater on Mars, *Icarus*, *159*(1), 53–73.

Burr, D. M., P. A. Carling, R. A. Beyer, and N. Lancaster (2004), Flood-formed dunes in Athabasca Valles, Mars: Morphology, modelling and implications, *Icarus*, *171*(1), 68–83.

Carr, M. H. (1979), Formation of Martian flood features by release of water from confined aquifers, *J. Geophys. Res.*, *84*(B6), 2995–3007.

Carr, M. H. (1986), Mars: A water-rich planet?, *Icarus*, *68*(2), 187–216.

Carr, M. H., and G. D. Clow (1981), Martian channels and valleys: Their characteristics, distribution, and age, *Icarus*, *48*(1), 91–117.

Chapman, M. G., and D. H. Scott (1989), Geology and hydrology of the North Kasei Valles area, *Mars, Proc. Lunar Planet. Sci. Conf.*, *19th*, 367–375.

Chapman, M. G., and K. L. Tanaka (1990), Small valleys and hydrologic history of the lower Mangala Valles region, Mars, *Proc. Lunar Planet. Sci. Conf., 20th*, 531–539.

Chapman, M. G., and K. L. Tanaka (1993), Geologic map of the MTM -05152 and -10152 quadrangles, Mangala Valles region of Mars, *Ser. Map, I-2294*, scale 1:500,000, U.S. Geol. Surv. Misc. Invest. Serv., Reston, Va.

Chapman, M. G., and K. L. Tanaka (2002), Related magma-ice interactions: Possible origins of chasmata, chaos, and surface materials in Xanthe, Margaritifer, and Meridiani Terrae, Mars, *Icarus*, *155*(2), 324–339.

Chapman, M. G., M. T. Gudmundsson, A. J. Russell, and T. M. Hare (2003), Possible Juventae Chasma subice volcanic eruptions and Maja Valles ice outburst floods on Mars: Implications of Mars Global Surveyor crater densities, geomorphology, and topography, *J. Geophys. Res.*, *108*(E10), 5113, doi:10.1029/2002JE002009.

Clifford, S. M. (1993), A model for the hydrologic and climatic behavior of water on Mars, *J. Geophys. Res.*, *98*(E6), 10,973–11,016.

Clifford, S. M., and T. J. Parker (2001), The evolution of the Martian hydrosphere: Implications for the fate of a primordial ocean and the current state of the northern plains, *Icarus*, *154*(1), 40–79.

Coleman, N. M. (2005), Martian mega-flood-triggered chaos formation, revealing groundwater depth, cryosphere thickness, and crustal heat flux, *J. Geophys. Res.*, *110*, E12S20, doi:10.1029/2005JE002419.

Costard, F., J. Aguirre-Puente, R. Greeley, and N. Makhloufi (1999), Martian fluvial-thermal erosion: Laboratory simulation, *J. Geophys. Res.*, *104*(E6), 14,091–14,098.

Craddock, R. A., and R. Greeley (1994), Geologic map of the MTM-20147 Quadrangle, Mangala Vallis region of Mars, *Map I-2310*, *U.S. Geol. Surv., Misc. Invest. Serv.*, Reston, Va.

Edgett, K. S., and M. C. Malin (2000), New views of Mars eolian activity, materials, and surface properties: Three vignettes from the Mars Global Surveyor Mars Orbiter Camera, *J. Geophys. Res.*, *105*(E1), 1623–1650.

Ghatan, G. J., J. W. Head, and L. Wilson (2005), Mangala Valles, Mars: Assessment of early stages of flooding and downstream flood evolution, *Earth Moon Planets*, *96*(1–2), 1–57.

Golombek, M., and D. Rapp (1997), Size-frequency distribution of rocks on Mars and Earth analog sites: Implications for future landed missions, *J. Geophys. Res.*, *102*(E2), 4117–4129.

Golombek, M. P., A. F. C. Haldemann, N. K. Forsberg-Taylor, E. N. DiMaggio, R. D. Schroeder, B. M. Jakosky, M. T. Mellon, and J. R. Matijevik (2003), Rock size-frequency distributions on Mars and implications for Mars Exploration Rover landing safety and operations, *J. Geophys. Res.*, *108*(E12), 8086, doi:10.1029/2002JE002035.

Hanna, J. C., and R. J. Phillips (2005), Hydrological modeling of the Martian crust with application to the pressurization of aquifers, *J. Geophys. Res.*, *110*, E01004, doi:10.1029/2004JE002330.

Hanna, J. C., and R. J. Phillips (2006), Tectonic pressurization of aquifers in the formation of Mangala and Athabasca Valles, Mars, *J. Geophys. Res.*, *111*, E03003, doi:10.1029/2005JE002546.

Hartmann, W. K. (1974), Geological observations of Martian arroyos, *J. Geophys. Res.*, *79*(26), 3951–3957.

Head, J. W., III, D. R. Marchant, and G. J. Ghatan (2004), Glacial deposits on the rim of a Hesperian-Amazonian outflow channel source trough: Mangala Valles, Mars, *Geophys. Res. Lett.*, *31*, L10701, doi:10.1029/2004GL020294.

Kleinhans, M. G. (2005), Flow discharge and sediment transport models for estimating a minimum timescale of hydrological activity and channel and delta formation on Mars, *J. Geophys. Res.*, *110*, E12003, doi:10.1029/2005JE002521.

Kochel, R. C., and J. F. Piper (1986), Morphology of large valleys on Hawaii: Evidence for groundwater sapping and comparisons with Martian valleys, *Proc. Lunar Planet. Sci. Conf. 17th*, Part 1, *J. Geophys. Res.*, *91*(B13), E175–E192.

Komar, P. D. (1979), Comparisons of the hydraulics of water flows in Martian outflow channels with flows of similar scale on Earth, *Icarus*, *37*(1), 156–181.

Komar, P. D. (1980), Modes of sediment transport in channelized water flows with ramifications to the erosion of the Martian outflow channels, *Icarus*, *42*(3), 317–329.

Komar, P. D. (1983), Shapes of streamlined islands on Earth and Mars: Experiments and analysis of the minimum-drag form, *Geology*, *11*, 651–654.

Komar, P. D. (1984), The lemniscate loop-comparisons with the shapes of streamlined landforms, *J. Geol.*, *92*, 133–145.

Laity, J. E., and M. C. Malin (1985), Sapping processes and the development of theater-headed valley networks on the Colorado Plateau, *Geol. Soc. Am. Bull.*, *96*, 203–217.

Leask, H. J. (2005), Volcano-ice interactions and related geomorphology at Mangala Valles and Aromatum Chaos, Mars, M. Phil. thesis, 199 pp., Lancaster Univ., Lancaster, U. K.

Leask, H. J., L. Wilson, and K. L. Mitchell (2006a), Formation of Ravi Vallis outflow channel, Mars: Morphological development, and water discharge and duration estimates, *J. Geophys. Res.*, *111*, E08070, doi:10.1029/2005JE002550.

Leask, H. J., L. Wilson, and K. L. Mitchell (2006b), Formation of Aromatum Chaos, Mars: Morphological development as a result of volcano-ice interactions, *J. Geophys. Res.*, *111*, E08071, doi:10.1029/2005JE002549.

Leask, H. J., L. Wilson, and K. L. Mitchell (2007), Formation of Mangala Fossa, the source of the Mangala Valles, Mars: Morphological development as a result of volcano-cryosphere interactions, *J. Geophys. Res.*, *112*, E02011, doi:10.1029/2005JE002644.

Luo, W., R. E. Arvidson, M. Sulton, R. Becker, M. K. Crombie, N. Sturchio, and Z. El Alfy (1997), Ground-water sapping processes, western desert, Egypt, *Geol. Soc. Am. Bull.*, *109*, 43–62.

Manga, M. (2004), Martian floods at Cerberus Fossae can be produced by groundwater discharge, *Geophys. Res. Lett.*, *31*, L02702, doi:10.1029/2003GL018958.

Mars Channel Working Group (1983), Channels and Valleys of Mars, *Geol. Soc. Am. Bull.*, *94*, 1035–1054.

Masursky, H., J. M. Boyce, A. L. Dial, G. G. Schaber, and M. E. Strobel (1977), Classification and time of formation of Martian channels based on Viking data, *J. Geophys. Res.*, *82*(28), 4016–4038.

Nummedal, D., and D. B. Prior (1981), Generation of Martian chaos and channels by debris flows, *Icarus*, *45*(1), 77–86.

Nummedal, D., J. J. Gonsiewski, and J. C. Boothroyd (1976), Geological significance of large channels on Mars, *Geol. Romana*, *15*, 407–418.

Rice, J. W., P. R. Christensen, M. C. Malin, and A. S. McEwen (2002), THEMIS observations of fluvial landforms on Mars, *Eos. Trans. AGU*, *83*(47), Fall Meet. Suppl., P11B-08.

Schultz, P. H., R. A. Schultz, and J. Rogers (1982), The structure and evolution of ancient impact basins on Mars, *J. Geophys. Res.*, *87*(B12), 9803–9820.

Scott, D. H., and K. L. Tanaka (1986), Geologic map of the western equatorial region of Mars, *Map I-1802-A*, *U.S. Geol. Surv., Misc. Invest. Serv.*, Reston, Va.

Sharp, R. P., and M. C. Malin (1975), Channels on Mars, *Geol. Soc. Am. Bull.*, *86*, 593–609.

Squyres, S. W. (1984), The history of water on Mars, *Annu. Rev. Earth Planet. Sci.*, *12*, 83–106.

Tanaka, K. L. (1986), The stratigraphy of Mars, *Proc. Lunar Plan. Sci. Conf., 17th*, Part 1, *J. Geophys. Res.*, *91*(B13), E139–E158.

Tanaka, K. L., and M. G. Chapman (1990), The relation of catastrophic flooding of Mangala Valles, Mars, to faulting of Memnonia Fossae and Tharsis volcanism, *J. Geophys. Res.*, *95*(B9), 14,315–14,323.

Theilig, E., and R. Greeley (1979), Plains and channels in the Lunae Planum-Chryse Planitia region of Mars, *J. Geophys. Res.*, *84*(B14), 7994–8010.

Trevena, A. S., and M. D. Picard (1978), Morphometric comparison of braided Martian channels and some braided Terrestrial features, *Icarus*, *35*(3), 385–394.

U.S. Geological Survey (2003), Gazetteer of planetary nomenclature, http://planetarynames.wr.usgs.gov/, Flagstaff, Ariz.

Wallace, D., and C. Sagan (1979), Evaporation of ice in planetary atmospheres: Ice-covered rivers on Mars, *Icarus*, *39*(3), 385–400.

Wilson, L., and J. W. Head III (2002), Tharsis-radial graben systems as the surface manifestation of plume-related dike intrusion complexes: Models and implications, *J. Geophys. Res.*, *107*(E8), 5057, doi:10.1029/2001JE001593.

Wilson, L., and J. W. Head III (2004), Evidence for a massive phreatomagmatic eruption in the initial stages of formation of the Mangala Valles outflow channel, Mars, *Geophys. Res. Lett.*, *31*, L15701, doi:10.1029/2004GL020322.

Wilson, L., G. J. Ghatan, J. W. Head III, and K. L. Mitchell (2004), Mars outflow channels: A reappraisal of the estimation of water flow velocities from water depths, regional slopes and channel floor properties, *J. Geophys. Res.*, *109*, E09003, doi:10.1029/2004JE002281.

Zimbelman, J. R., R. A. Craddock, R. Greeley, and R. O. Kuzmin (1992), Volatile history of Mangala Valles, Mars, *J. Geophys. Res.*, *97*(E11), 18,309–18,317.

Zimbelman, J. R., R. A. Craddock, and R. Greeley (1994), Geologic map of the MTM-15147 quadrangle, Mangala Valles region of Mars, *Ser. Map, I-2402*, scale 1:500,000, *U.S. Geol. Surv., Misc. Invest. Serv.*, Reston, Va.

H. J. Leask and L. Wilson, Planetary Science Research Group, Environmental Science Department, Institute of Environmental and Natural Sciences, Lancaster University, Lancaster LA1 4YQ, UK. (l.wilson@lancaster.ac.uk)

K. L. Mitchell, Jet Propulsion Laboratory, Mail Stop 183-601, 4800 Oak Grove Drive, Pasadena, CA 91109-8099, USA.